

Vapor-fed microfluidic hydrogen generator

(Electronic Supplementary Information)

M.A. Modestino, M. Dumortier, S.M. Hosseini Hashemi, S. Haussener, C. Moser and D. Psaltis.

School of Engineering, École Polytechnique Fédéral de Lausanne (EPFL)

1. Modelling results for gas crossover

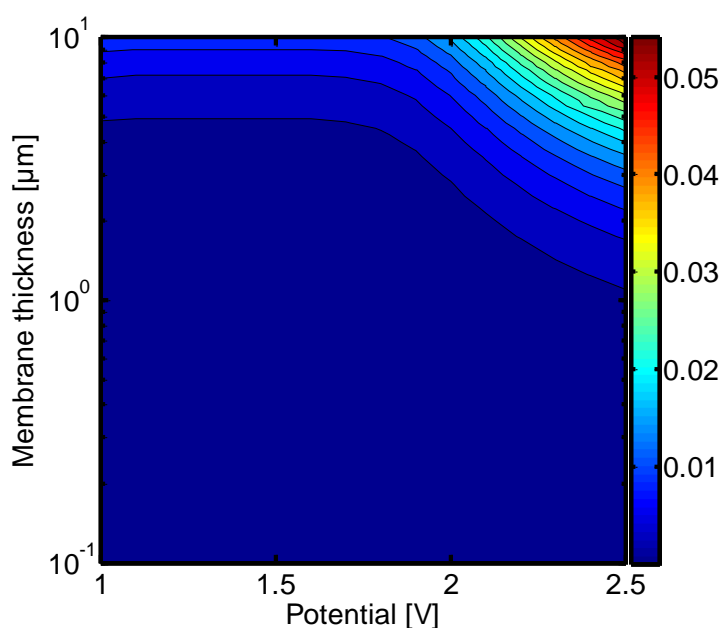


Figure S1. Hydrogen crossover flow between the cathode and the anode as a fraction of the hydrogen production rate at the cathode. The results show that the gas crossover across electrodes is expected to be low, in the order of 10^{-3} of the produced hydrogen.

2. Gas Chromatography Traces

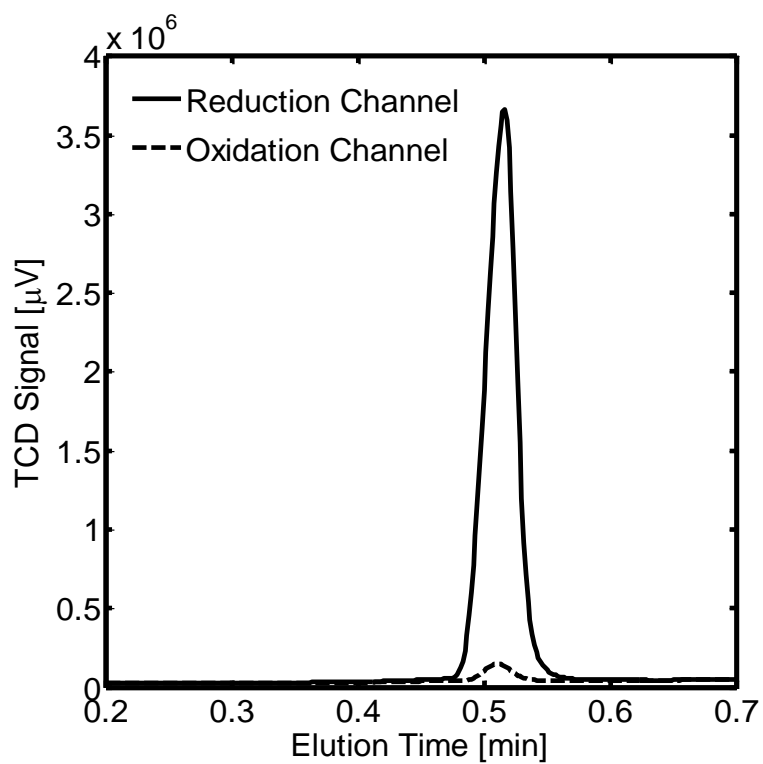


Figure S2. Gas chromatography traces for H_2 collected in the oxidation and reduction channel, showing small amounts of H_2 crossover between channels.

3. PEIS Measurement of devices at steady state

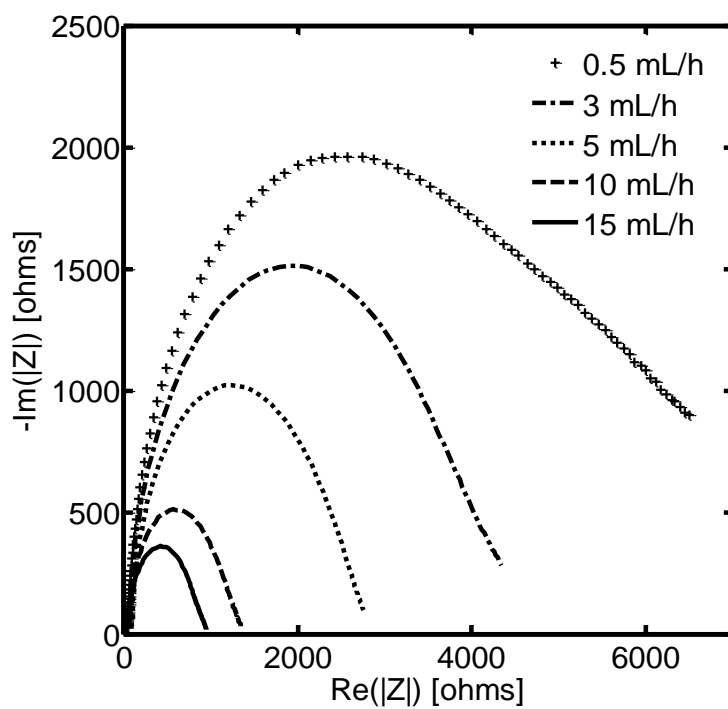


Figure S3. PEIS measurements on devices under different feed flowrates after 15 min of device operation at 3 V. The impedance spectra demonstrates an increase film resistance as the flowrate was reduced in the devices

4. Microelectrodes operated under liquid electrolytes

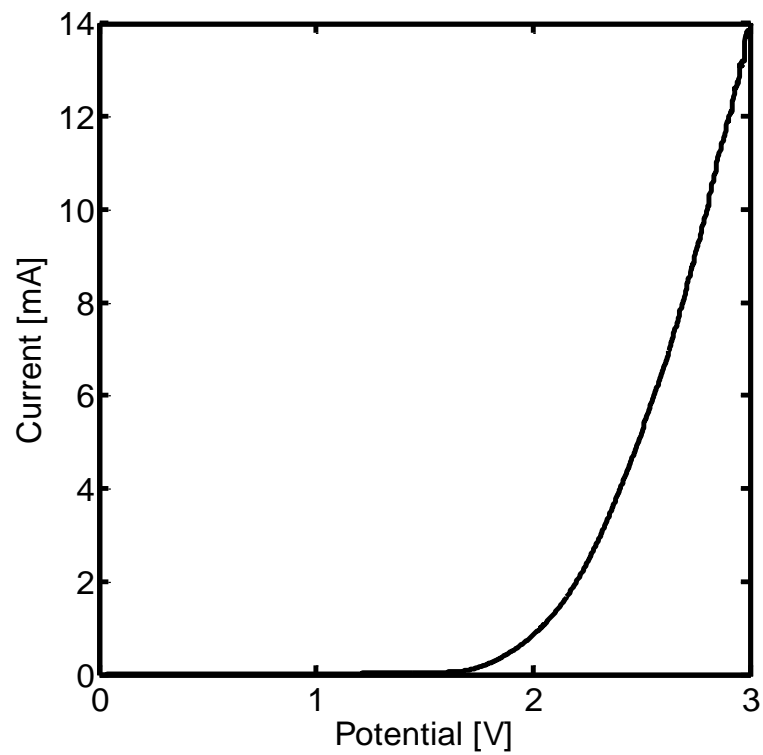
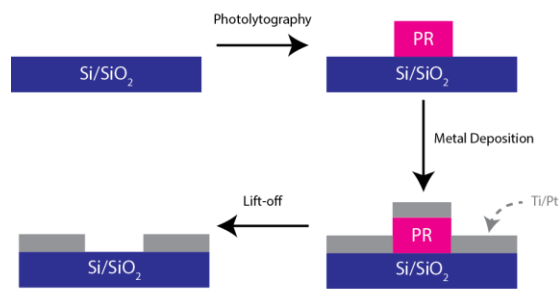


Figure S4. Microelectrolyzer load curve obtained for electrodes operated under 1M sulfuric acid solution. The current densities achieved under liquid electrolytes are higher than from vapor feeds as the transport limitations are alleviated.

5. Microfabrication process flow diagram

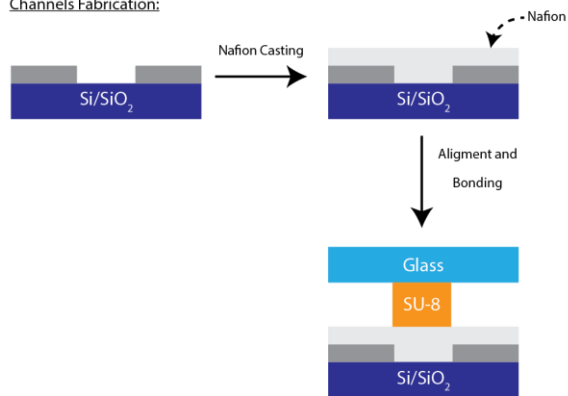
Microelectrode Fabrication:



Channels Fabrication:



Channels Fabrication:



Mixed Catalyst Microelectrode Fabrication:

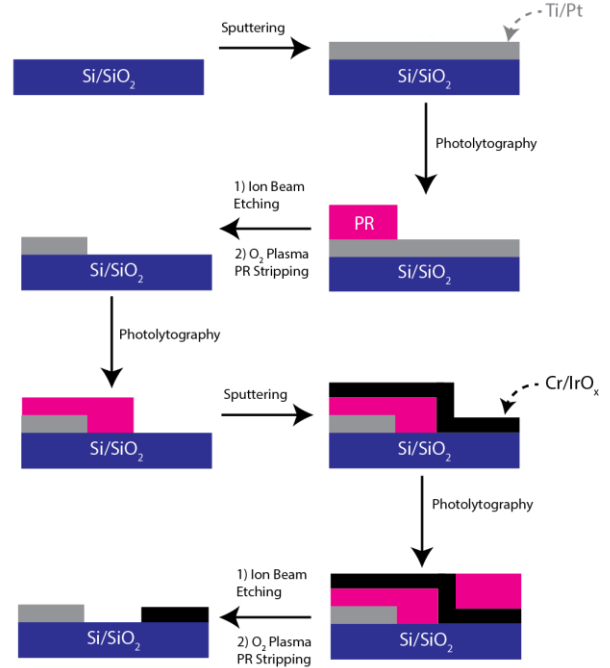


Figure S5. Process flow diagram for microfabrication of vapor-fed electrolyzers

6. Electrode design used for fabrication of microfluidic devices

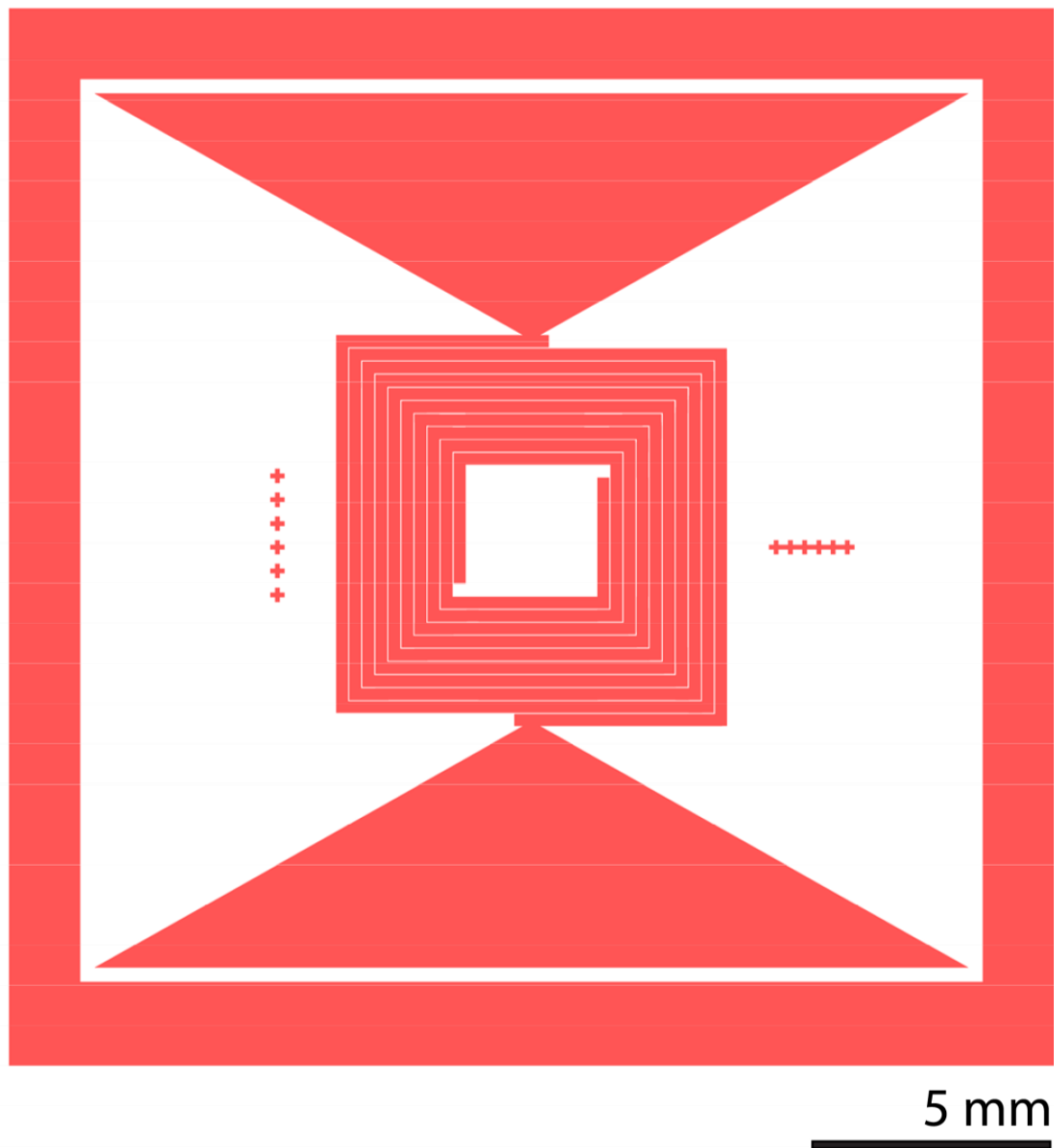


Figure S6. Diagram of pattern used for fabrication of microelectrode array

7. Catalyst surface characterization

The surface area of the electrodes was determined by atomic force microscopy using Bruker Dimension FastScan System (Figure S7). By analyzing the obtained data, it was determined that the surface area of the catalyst was only 6.1% higher than its projected area. The root mean square roughness of the sample was determined to be 2.2 nm.

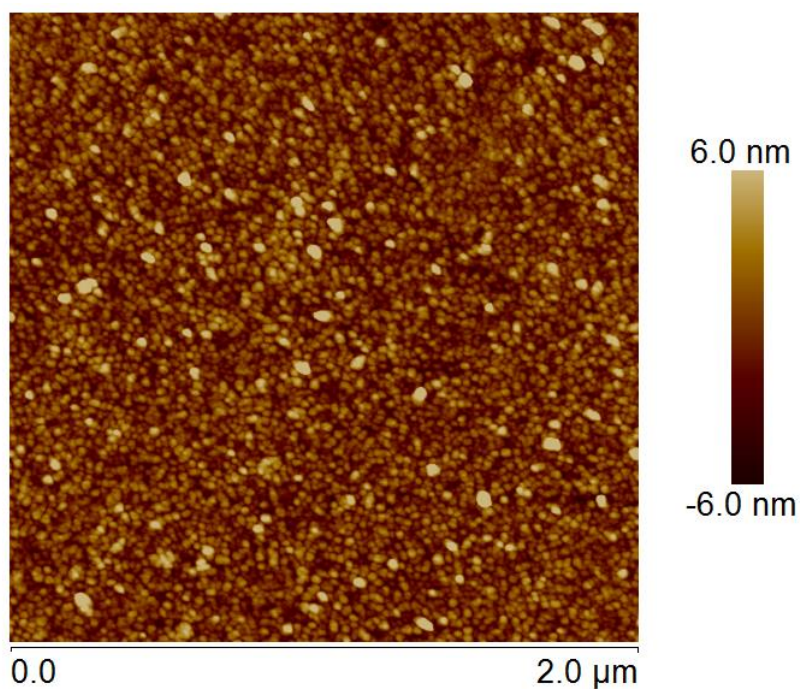


Figure S7. Atomic force microscopy image of the surface of Platinum electrocatalyst.

8. Energy conversion efficiency under humid N₂

The energy conversion efficiency (η) was estimated for the device operated under humid N₂, assuming a 100% faradaic efficiency. η was calculated as,

$$\eta = \frac{E_{H_2O,vap}^0}{E_{app}}$$

Where E_{app} is the applied potential and $E_{H_2O,vap}^0$ is the thermodynamic water splitting potential of water vapor.[1]

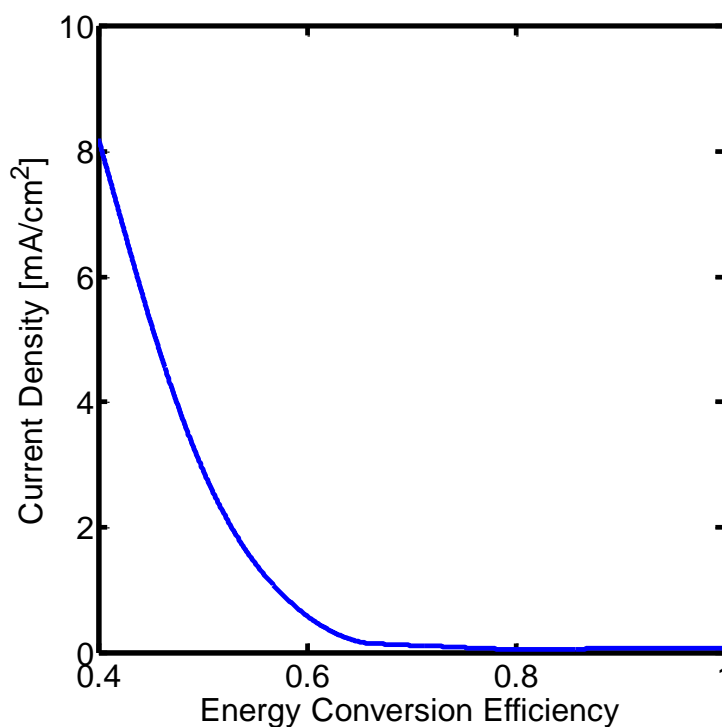


Figure S8. Current density versus energy conversion efficiency for a microelectrolyzer device consisting of a pair of Platinum electrodes and operated under humid N₂ streams at 100%RH.

9. References

1. Spurgeon, J.M. and N.S. Lewis, *Proton exchange membrane electrolysis sustained by water vapor*. Energy & Environmental Science, 2011. 4(8): p. 2993-2998.